Evaluation of Traveling Wave-Based Fault Location Methods Applied to HVDC Systems

P. C. Fernandes, H. N. G. V. Gonçalves, K. M. Silva, F. V. Lopes

***Abstract*—This paper presents an evaluation of traveling wave (TW)-based fault location methods when applied to High Voltage Direct Current (HVDC) system. The tests are carried out using a bipole HVDC link, which was modeled and simulated by means of the Alternative Transients Program (ATP). Pole-to-ground and pole-pole fault scenarios were analyzed and four TW-based fault location approaches were implemented. Modal transformation was used to decouple the bipole current signals and, then, the Differentiator-Smoother (DS) filter was applied to allow an accurate TW arrival time detection at the monitored HVDC link terminals. The evaluated algorithms showed good accuracy in face of fault position and fault resistance variations. Also, in cases of inaccuracies in line parameters, only settings-free methods based on unsynchronized data remained precise.**

***Keywords*—HVDC, traveling waves, fault location, transmission lines, electromagnetic transients, power systems.**

I. Introduction

THE constant developments on power electronics made HVDC transmission feasible in today‘s technology, offering an alternative for bulk power transmission over long distances with lower costs and no reactive compensation throughout the lines [1].

Due to the their lengths, long HVDC transmission lines pass through very distinct environments and, consequently, they have higher probability of maloperation due to faults [2]. Therefore, locating faults in a fast and accurate way is of utmost importance for HVDC links, because it quickens maintenance groups actions and guarantees faster electrical energy restoration to the consumer.

In order to make this task possible, TW-based fault location methods originally proposed for AC transmission networks have been taken as feasible solutions for HVDC systems, mainly due to their line structure simplicity and to the fact that converter stations constrain the fault-induced TWs into the monitored line, facilitating the detection of wavefronts [3]–[5].

The conventional two-ended fault location method has been successfully applied in HVDC systems. This technique uses the first incident TWs arrival times at the converter stations to estimate the fault location. However, the need for data synchronization on both terminals and the line parameters dependence are some of the drawbacks of the method [6]–[10].

Another way to locate faults based on TWs is using one-ended fault location methods. These methods are based on the arrival times of the first incident TW and its consecutive reflection that comes from the fault point to estimate the fault location. The main drawback of these methods is the need for distinguishing between TWs reflected from the fault and from other power system terminals, which can jeopardize the fault locator reliability [10], [11]. Also, the knowledge of line parameters is usually required to calculate the TWs propagation velocity, which is in turn used to estimate the fault distance, leading to fault location errors are expected in cases of uncertainties in line parameters [9].

A different approach to locate faults using TWs is applying a fault location method based on aerial and ground modes [10], [12]. By doing so, only the first aerial and ground mode TWs are required to be detected, so that the need for data synchronization, line parameters or the detection of reflected wave-fronts can be eliminated, depending on the used approach.

Although several TW-based fault location solutions for AC transmission lines have been reported over the recent decades, studies on the performance of these methods when applied to HVDC links are still scarce in the literature. Thus, this paper evaluates different TW-based fault location methods applied to HVDC systems aiming to identify advantages and limitations due to the line terminations characteristics (converter stations, smoothing reactors and DC filters).

The performance of each technique is evaluated in different fault scenarios (pole-to-ground and pole-pole) by means of ATP simulations, in which fault distance throughout the HVDC line, fault resistance and uncertainties in line parameters were varied. From the obtained results, it is demonstrated that traditional TW-based fault location methods originally developed for AC systems are also able to provide accurate fault distance estimations in HVDC links, yielding errors of the order of a typical tower span.

II. TW-Based Fault Location Algorithm

In this paper, four TW-based fault location formulations are assessed by means of tests in a bipole HVDC link. To do so, the fault location procedure was accomplished using the same algorithm for all formulations, which can be divided in three steps: A) Modal Transformation, B) Traveling Wave Arrival Time Extraction, C) Fault Distance Estimation.

A. Modal Transformation

It is known that multi-phase power systems are mutually coupled and, therefore, a single TW propagation velocity does not exist [8]. To overcome the coupling, it is possible to fully decouple the power system using transformation matrices, taking the transmission line models as fully transposed.

This study was financed in part by the Coordenação de Aperfeiçoamento de Pessoal de Nível Superior - Brasil (CAPES) - Finance Code 001.

Paper submitted to the International Conference on Power Systems Transients (IPST2019) in Perpignan, France June 16-20, 2019.

Analogously, a HVDC bipole can be seen as a two-phase system. Then, if a transformation matrix designed for a two-phase system is applied to a HVDC bipole, it will be equally decoupled [13]. This paper uses the Karrenbauer transformation matrix T below:

$$T = \frac{1}{2}\begin{bmatrix} 1 & 1 \\ 1 & -1 \end{bmatrix}, \tag{1}$$

being the modal currents and voltages given by:

$$\begin{bmatrix} i_0 \\ i_1 \end{bmatrix} = T \begin{bmatrix} v_+ \\ v_- \end{bmatrix}, \tag{2}$$

$$\begin{bmatrix} v_0 \\ v_1 \end{bmatrix} = T \begin{bmatrix} i_+ \\ i_- \end{bmatrix}, \tag{3}$$

where v_+, v_- are the positive and negative pole voltages, i_+, i_- are the positive and negative pole currents, v_0, v_1 are the ground and aerial mode voltages and i_0, i_1 are the ground and aerial mode currents.

Conventional two- and one-ended TW fault location methods normally use aerial mode current signals only, because it presents less attenuation and dispersion [14]. Here, the same is considered.

B. Traveling Wave Arrival Time Extraction

TW arrival time extraction is key to the accuracy of TW-based fault locators. The most widespread technique is the wavelet transform, due to its simultaneous time and frequency localization capabilities. However, its performance depends on the chosen mother wavelet [15], so that previous studies are required to define the filter coefficients.

As a result, several techniques have been conducted toward finding reliable TW detection methods, such as the Differentiator-Smoother (DS) filter, a technique first implemented on [16], [17] aiming to locate faults on a DC line and that has been successfully applied in real-world systems for TW-based fault location and time-domain protection [14]. In this paper, the DS filter is applied.

Figure 1 presents the DS filter response to a step- and ramp-like current input signals. For input step-changes, the DS filter responds with a triangle-shaped output, whereas for ramp-like input signals, a parabola-shaped output is obtained. In both cases, after filtering the input signal, the arrival times must be accurately detected.

These instants are mapped by applying a threshold to the filtered signal, followed by the output peak detection. The detection is performed by comparing the output peak value to a hard-threshold, which is set based on the system features [18]. Then, a spline interpolation is applied few samples around the peak value to optimize the arrival time estimation [14].

C. Fault Distance Estimation

1) Conventional Two-Ended Method: As described in previous sections, the two-ended fault location method detects the first aerial mode TWs at both line terminals (rectifier and inverter sides). Drawing the lattice diagram of TWs coming from the fault point on Figure 2, one can derive the fault

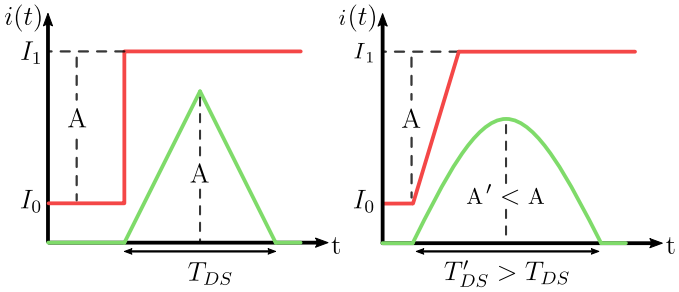

Fig. 1. DS filter response to a step-like input current $i(t)$.

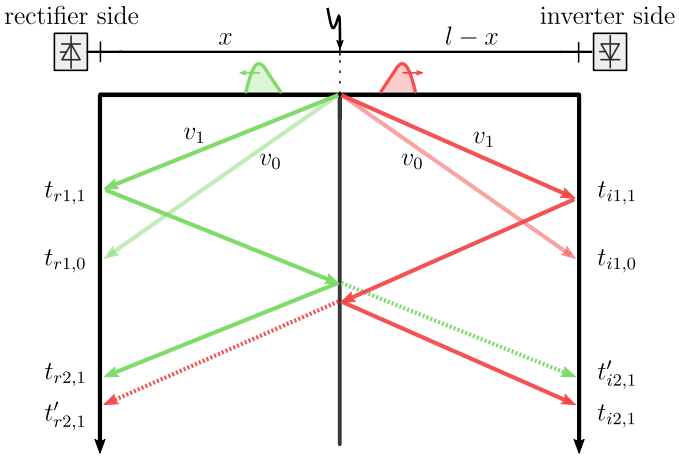

Fig. 2. Lattice diagram of traveling waves generated from the fault point.

location $\tilde{x}$ based on aerial mode TW arrival times $t_{r1,1}$ and $t_{i1,1}$, aerial mode propagation velocity v_1 and line length l as:

$$\tilde{x} = \frac{v_1(t_{r1,1} - t_{i1,1}) + l}{2}. \tag{4}$$

2) Conventional One-Ended Method: One-ended fault location method uses the first and second aerial mode TWs at the monitoring terminal (rectifier side, for example) and, based on its arrival times $t_{r1,1}$ and $t_{r2,1}$ and aerial mode propagation velocity v_1 on Figure 2, it estimates the fault location $\tilde{x}$ as:

$$\tilde{x} = \frac{v_1(t_{r2,1} - t_{r1,1})}{2}. \tag{5}$$

Equation (5) shows that one-ended methods do not use line length l information to estimate $\tilde{x}$. Besides, regarding the above mentioned issue on distinguishing between TWs reflected from the fault and from power system terminals, if the fault takes place at the transmission line's second half $l-x$ far from the inverter side, the formulation changes to:

$$\tilde{x} = l - \frac{v_1(t'_{r2,1} - t_{r1,1})}{2}, \tag{6}$$

where $t'_{r2,1}$ represents the arrival time of the second aerial mode TW reflected back from the inverter side terminal.

It is important to emphasize that the origin of the second TW varies from being reflected from the fault point to being reflected from the non-monitoring terminal (inverter side) and, afterwards, transmitted from the fault point.

Other issue to be commented regards the line terminations, which has influence on the polarity of TWs reflected at the

monitoring terminal. As a result, difficulties on determining the polarity of TWs reflected from the fault point are usually reported. On the other hand, in HVDC lines, unlike AC systems, the features of local and remote converter stations are usually known, facilitating the detection of wave-fronts reflected from the fault point.

3) One-Ended Modal Method: The one-ended modal fault location method reported in [12] utilizes the first aerial and ground mode TWs at the monitoring terminal (rectifier side, for example) and, combining its arrival times $t_{r1,1}$, $t_{r1,0}$ with its aerial and ground mode propagation velocities v_1 and v_0, the fault location $\tilde{x}$ is derived:

$$\tilde{x} = \frac{v_0 v_1 (t_{r1,0} - t_{r1,1})}{(v_1 - v_0)} \ . \tag{7}$$

In (7), it is noticed that the line length l is not used, but now the method not only depends on aerial mode propagation velocity v_1, but also on ground mode propagation velocity v_0.

4) Two-Ended Modal Method: The two-ended modal fault location method reported in [10] uses the first aerial and ground mode TWs at each monitoring terminal and, again, based on its arrival times $t_{r1,1}$, $t_{r1,0}$, $t_{i1,1}$ and $t_{i1,0}$ on Figure 2, calculates the fault distance estimation $\tilde{x}$ as:

$$\tilde{x} = \frac{t_{r1,0} - t_{r1,1}}{(t_{r1,0} - t_{r1,1}) + (t_{i1,0} - t_{i1,1})} \cdot l \ . \tag{8}$$

Equation (8) does not rely on propagation velocities v_0 and v_1, diminishing errors provided by these quantities. Besides, line length l information is required only to calculate fault distance estimations in kilometers, so that its knowledge is not required if per unit fault distance estimations are computed.

III. HVDC System Benchmark

The HVDC system benchmark utilized to verify the performance of TW-based fault location techniques described so far was modeled in [19] using the ATP/ATPDraw software and it was based on a transcription from an initial reference made using the PSCAD software to provide technical studies on HVDC transmission systems to the brazilian Energy Planning Company (EPE). A simplified scheme of the ATP/ATPDraw version in [19] is shown in Figure 3 and it stands for the Madeira River HVDC link, which is constituted of two bipoles (3150 MW and $\pm$ 600 kV each) that interconnect two stations, Coletora Porto Velho (Brazil) and Araraquara II (Brazil). The rated current is 2625 A and the line length is 2450 km. The HVDC system benchmark uses a fully transposed line model, with distributed and frequency independent parameters, which are are summarized on Figure 4 and Table I [19].

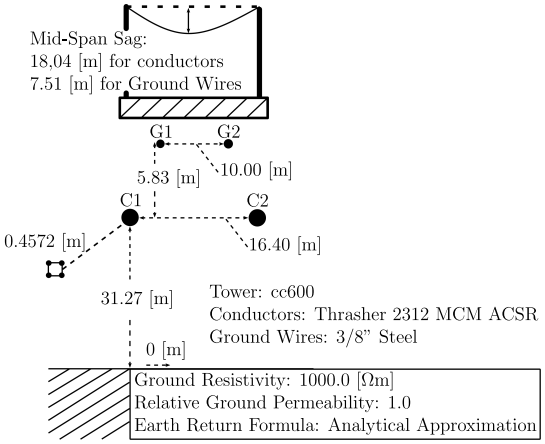

Fig. 4. HVDC tower parameters presented in [19].

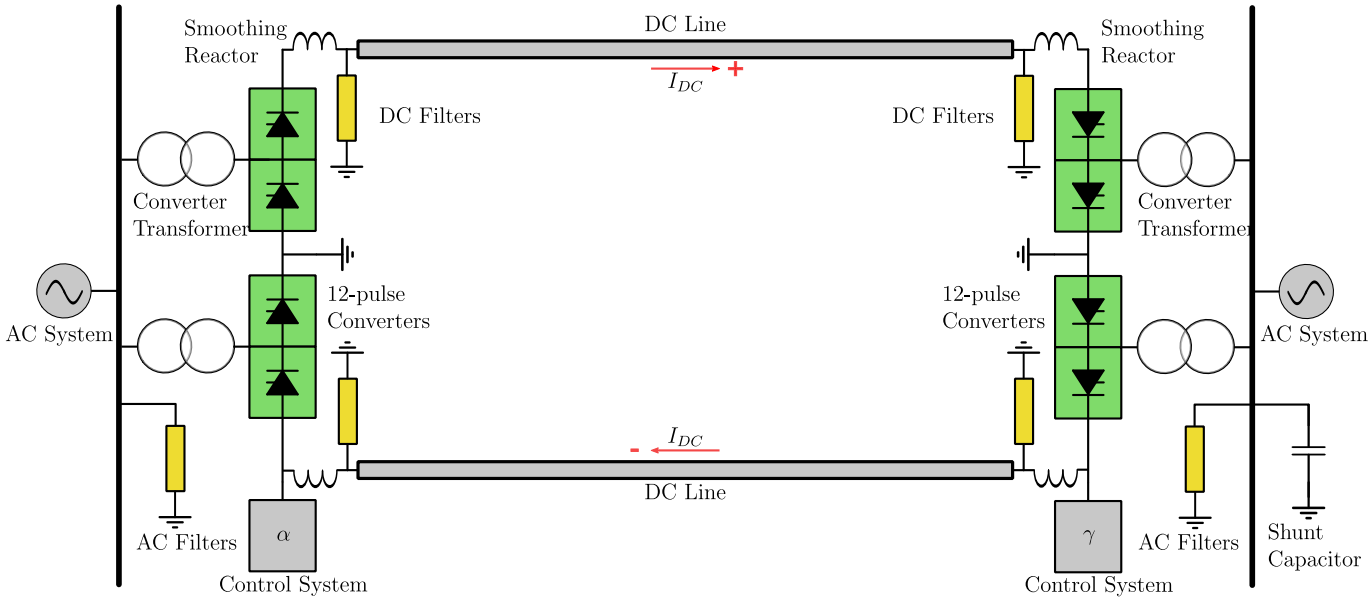

Fig. 3. Single-line diagram of a HVDC bipole and its components.

TABLE I
HVDC TRANSMISSION LINE PARAMETERS.

Aerial Mode			Ground Mode		
R'(Ω/km)	L'(mH/km)	C'(μF/km)	R'(Ω/km)	L'(mH/km)	C'(μF/km)
0.00702	0.860602	0.0134166	0.008028	3.88784	0.0100794

IV. PERFORMANCE EVALUATION

The fault scenarios simulated at 1 MHz on the ATP model of the Madeira River Bipole were: pole-to-ground fault on the positive pole and a pole-pole fault, in which the TW detection algorithm was set with thresholds equal to 100 amperes and 150 amperes, respectively. Each scenario passed through three specific fault location performance tests.

The first test scenario varies the fault distance from 1% to 99%, with steps of 1% and fixed fault resistance (R_f = 1 Ω for pole-to-ground and R_f = 20 Ω for pole-pole). The second test adds line parameters inaccuracies, representing possible weather and climatic conditions due to the extension of the line simulated by adding +10% error on aerial and ground mode line inductances L_0 and L_1 and varying again the fault distance. The last scenario varies fault resistance R_f from 0 Ω to 1000 Ω, with steps of 100 Ω, considering a fixed fault distances at 25, 50 and 75% of the line length.

To rate the precision associated with each method, the absolute error was calculated as follows:

$$\varepsilon_{abs} = |\tilde{x} - x| \ , \tag{9}$$

where $\tilde{x}$ and x are the estimated and actual fault distances.

A. Pole-to-Ground Fault Cases

1) Fault Location Variations: To rate each TW fault location method accuracy, the cumulative frequency polygon technique was utilized and its outcome is illustrated on Figure 5. The higher the slope of the obtained curves, the better the method accuracy, because it maps a greater range of cases within smaller absolute errors. Therefore, the two-ended modal fault location method showed best accuracy overall.

On the other hand, one-ended modal fault location methods and the conventional two-ended method presented greater variations in accuracy. These variations are mainly related to the different levels of dispersion verified in the wave-fronts that reach both line terminals as well as in the incident and reflected TWs, resulting in time displacements of the DS filter output peak position [14].

It is noteworthy to emphasize that the greater the fault distance from the monitoring terminals, the greater the dispersion effect. Since one-ended fault location methods extract waves from only one terminal, the dispersion rises as the fault gets away from monitoring terminal. The two-ended method extracts waves from both terminals, so there will always be one terminal closer to the fault and the other one more distant from the fault, creating dispersion at some level.

These issues result in additional errors, which are less prominent in typical AC transmission lines with lengths of about few hundreds of kilometers. On Table II, the mean and maximum absolute errors of each method is presented, showing that, overall, performance is good.

In fact, the greatest mean absolute error, obtained from two-ended method, is 184.24 m, whereas the maximum absolute error, obtained from one-ended modal method (inverter side), is of about 659.05 m. The most accurate technique was the two-ended modal method, whose maximum absolute error did not exceed 514.50 m. Even so, analyzing all computed errors, they did not exceed 700 m, being smaller than three conventional tower spans (≈ 900 m).

2) Line Parameters Inaccuracies: The effect of adding line parameters inaccuracies on each fault location method is shown on Table III. All methods showed to be impacted by adding +10% error on aerial and ground mode line inductances L_0 and L_1, except the two-ended modal method which is settings-free. The errors are associated to the dependence on these methods to the propagation velocities v_0 and/or v_1,

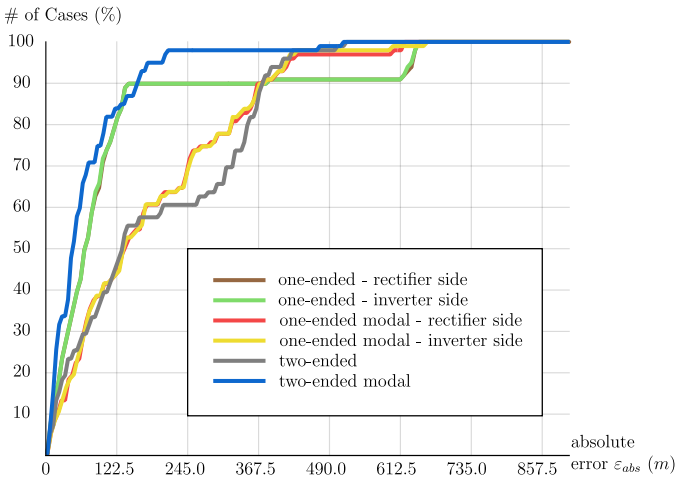

Fig. 5. Cumulative frequency polygon technique applied on fault location variations - Pole-to-Ground fault.

TABLE II
MEAN AND MAXIMUM ABSOLUTE ERRORS (M) OF TW FAULT LOCATION METHODS FOR THE MADEIRA RIVER BIPOLE - POLE-TO-GROUND FAULT, FAULT LOCATION VARIATIONS.

Method	Mean (m)	Max (m)
One-Ended - Rectifier Side	116.38	641.90
One-Ended - Inverter Side	115.89	641.90
One-Ended Modal - Rectifier Side	177.14	617.40
One-Ended Modal - Inverter Side	174.93	659.05
Two-Ended	184.24	519.40
Two-Ended Modal	67.62	514.50

TABLE III
MEAN AND MAXIMUM ABSOLUTE ERRORS (KM) OF TW FAULT LOCATION METHODS FOR THE MADEIRA RIVER BIPOLE - POLE-TO-GROUND FAULT, LINE PARAMETERS INACCURACIES.

Method	Mean (km)	Max (km)
One-Ended - Rectifier Side	2.87	5.69
One-Ended - Inverter Side	2.87	5.69
One-Ended Modal - Rectifier Side	5.70	11.26
One-Ended Modal - Inverter Side	5.70	11.26
Two-Ended	2.81	5.55
Two-Ended Modal	0.068	0.052

parameters that are directly affected by changes on L_0, L_1.

3) Fault Resistance Variations: To comprehend the impacts of fault resistance R_f variations, three faults were applied at 25%, 50% and 75% of the line length. For a fault occurring 25% away from the rectifier side, variations in R_f impacted the one-ended method with monitoring on the rectifier side. When $R_f = 200\ \Omega$, the error goes from 61.25 m to 515.90 km and, at 500 Ω, it goes to 1225.22 km. It means that TW detection errors occurred, which is a limitation of the transient detection algorithm rather than the fault location formula.

This limitation appears due to the rising of R_f, since the second TW coming towards the rectifier side suffers from attenuation on its amplitude, jeopardizing the fixed threshold imposed. Hence, the second TW is not detected on the correct time and the estimation misses the fault location.

Likewise, for a fault at 75% of the line, the one-ended fault location method with monitoring on the inverting side brings a similar inaccuracy on fault estimation: when $R_f = 200\ \Omega$, the error goes from 61.25 m to 515.90 km and at 400 Ω, it goes to 1225.22 km.

For a fault at 50% of the line, all fault location methods present small absolute errors, except for two-ended fault location methods which, by definition, have zero error estimation in the middle of the line.

Table IV shows the absolute error of the fault location methods, considering cases in which the TWs were properly detected. Disregarding cases in which methods suffered from attenuation, the estimations carry indeed small absolute errors.

B. Pole-Pole Fault Cases

1) Fault Location Variations: Analogously to the pole-to-ground fault, the cumulative frequency polygon technique was applied and the result is shown on Figure 6. Despite the fact of the slope presented by the two-ended fault location method being less than the one-ended methods, its maximum error, 519.40 m, is smaller than one-ended fault location methods, 641.90 m, since it reaches 100% of cases first. Table V shows that the behavior of estimation from the tested methods does not change from the pole-pole to the pole-to-ground fault scenario, since the mean and maximum absolute errors are kept the same.

2) Line Parameters Inaccuracies: Here, the behavior of tested fault location methods is analogous to what is presented on Section IV-A2. The mean and maximum absolute errors are also kept the same, as shown in Table VI.

TABLE IV
ABSOLUTE ERROR (M) OF TW FAULT LOCATION METHODS THROUGH THE 0-1000 Ω R_f RANGE FOR THE MADEIRA RIVER BIPOLE - POLE-TO-GROUND FAULT, FAULT RESISTANCE VARIATIONS.

Method	25% (m)	50% (m)	75% (m)
One-Ended - Rectifier Side	61.25*	138.43	54.64
One-Ended - Inverter Side	54.64	138.43	61.25*
One-Ended Modal - Rectifier Side	95.31	72.28	183.02
One-Ended Modal - Inverter Side	183.02	72.28	95.31
Two-Ended	85.51	0	85.51
Two-Ended Modal	25.73	0	25.73

*: absolute error varies throughout R_f range.

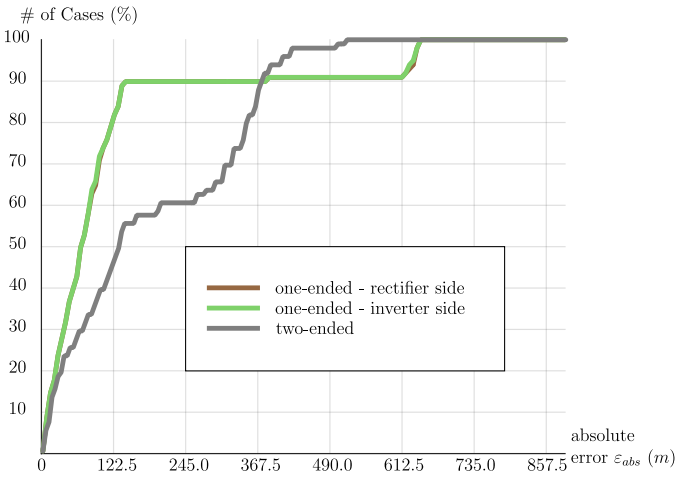

Fig. 6. Cumulative frequency polygon technique applied on fault location variations - Pole-Pole fault.

TABLE V
MEAN AND MAXIMUM ABSOLUTE ERRORS (M) OF TW FAULT LOCATION METHODS FOR THE MADEIRA RIVER BIPOLE - POLE-POLE FAULT, FAULT LOCATION VARIATIONS.

Method	Mean (m)	Max (m)
One-Ended - Rectifier Side	116.38	641.90
One-Ended - Inverter Side	115.89	641.90
Two-Ended	184.24	519.40

TABLE VI
MEAN AND MAXIMUM ABSOLUTE ERRORS (KM) OF TW FAULT LOCATION METHODS FOR THE MADEIRA RIVER BIPOLE - POLE-POLE FAULT, LINE PARAMETERS INACCURACIES.

Method	Mean (km)	Mean (km)
One-Ended - Rectifier Side	2.87	5.69
One-Ended - Inverter Side	2.87	5.69
Two-Ended	2.81	5.55

3) Fault Resistance Variations: For a fault occurring 25% away from the rectifier side, the methods kept good accuracy varying R_f. The one-ended method with monitoring on the rectifier side was more impacted when $R_f = 1000\ \Omega$, resulting in TW detection errors. Even so, in cases in which TWs were properly detected, errors of about 61.25 m were verified.

Now, the two-ended fault location method with monitoring on the inverter side, which was not affected on pole-to-ground faults, presented the opposite effect compared to the one-ended method referred to the rectifier side: at 0 Ω, the error is 1225.22 km, decreasing to 54.64 m from 100 Ω to 1000 Ω, exposing again the presence of TW detection errors.

The presence of a high error for a 0 Ω fault resistance is due to the pole-pole fault symmetry. In this case, pole-pole faults lead to a transmitted TW equals to zero from the fault point, given the circuit connections during the fault [20]. Since the second TW is coming from the rectifier side, when it passes through the fault, the TW is completely absorbed by the fault point, creating again a scenario which leads to TW detection errors.

For a fault at 75% of the line, the one-ended fault location method referred to the inverter side was more impacted when $R_f = 1000\ \Omega$, going from a 61.25 m to 1225.22 km error. The one-ended fault location method referred to the rectifier side started, at 0 Ω, with a 1225.22 km error that decreased to 54.64 m as R_f increased from 100 Ω to 1000 Ω.

For a fault at 50% of the line, one-ended fault location methods present small absolute errors, except for the two-ended method which, by definition, has zero error estimation in the middle of the line.

Table VII shows the absolute error of every method, considering only cases in which the TWs were properly detected. Again, disregarding TW detection errors, the presented estimations showed good results.

TABLE VII
ABSOLUTE ERROR (M) OF TW FAULT LOCATION METHODS THROUGH THE 0-1000 Ω R_f RANGE FOR THE MADEIRA RIVER BIPOLE - POLE-POLE FAULT, FAULT RESISTANCE VARIATIONS.

Method	25% (m)	50% (m)	75% (m)
One-Ended - Rectifier Side	61.25*	138.43	54.64*
One-Ended - Inverter Side	54.64*	138.43	61.25*
Two-Ended	85.51	0	85.51

*: absolute error varies throughout R_f range.

V. CONCLUSIONS

This paper presents an evaluation of fault location methods based on traveling waves theory applied to HVDC systems. In order to simulate the performance of each method, an ATP/ATPDraw software model of the Madeira River Bipole was tested on pole-to-ground and pole-pole fault scenarios. Both scenarios passed through three different sub-scenarios, fault distance variations, line parameters inaccuracies and fault resistance variations, in order to evaluate each fault location method performance.

In general, all the tested methods had good results for fault location variations, with mean absolute errors of $\approx$ 185 m, smaller than a conventional tower span ($\approx$ 300 m). Looking into the maximum absolute errors, all methods presented errors smaller than 700 m. Thus, for both pole-to-ground and pole-pole faults, the TW-based fault location methods showed good performance, favored by the termination characteristics of the HVDC link.

When line parameters inaccuracies were added to the system, all fault location methods dependent on propagation velocities are impacted, since their formulations utilize these parameters to estimate the fault location. Only the two-ended modal fault location method kept invariant facing these inaccuracies, showing a mean absolute error of 67.62 m.

Finally, taking into account variations on fault resistance, the transient detection algorithm showed TW detection errors in some cases. Disregarding the situations in which the TWs were not correctly detected, all fault location methods kept an estimation error compatible with a conventional tower span.

Future works look forward to improve the hard-threshold approach to correctly detect TWs, mainly second TWs detection due to amplitude attenuation, making it more generalist facing different faults by using different threshold and filtering techniques. Future works will also aim on establishing other test scenarios to study fault location methods performance on HVDC links, such as data synchronization inaccuracies.

REFERENCES

[1] E. W. Kimbark, *Direct current transmission*. John Wiley & Sons, 1971, vol. 1.

[2] Z. Ying, T. Nengling, and X. Bin, "Travelling wave-based pilot direction comparison protection for hvdc line," *International Transactions on Electrical Energy Systems*, vol. 23, no. 8, pp. 1304–1316, 2013.

[3] Y. Zhang, N. Tai, and B. Xu, "Fault analysis and traveling-wave protection scheme for bipolar hvdc lines," *IEEE Transactions on Power Delivery*, vol. 27, no. 3, pp. 1583–1591, 2012.

[4] X. Liu, A. Osman, and O. Malik, "Hybrid traveling wave/boundary protection for bipolar hcdc line," in *Power & Energy Society General Meeting, 2009. PES'09. IEEE*. IEEE, 2009, pp. 1–8.

[5] ——, "Hybrid traveling wave/boundary protection for monopolar hvdc line," *IEEE Transactions on Power Delivery*, vol. 24, no. 2, pp. 569–578, 2009.

[6] F. Lopes, K. Silva, F. Costa, W. Neves, and D. Fernandes, "Real-time traveling-wave-based fault location using two-terminal unsynchronized data," *IEEE Transactions on Power Delivery*, vol. 30, no. 3, pp. 1067–1076, 2015.

[7] P. Gale, P. Crossley, X. Bingyin, G. Yaozhong, B. Cory, and J. Barker, "Fault location based on travelling waves," in *Developments in Power System Protection, 1993., Fifth International Conference on*. IET, 1993, pp. 54–59.

[8] F. H. Magnago and A. Abur, "Fault location using wavelets," *IEEE Transactions on Power Delivery*, vol. 13, no. 4, pp. 1475–1480, 1998.

[9] M. M. Saha, J. J. Izykowski, and E. Rosolowski, *Fault location on power networks*. Springer Science & Business Media, 2009.

[10] F. V. Lopes, "Settings-free traveling-wave-based earth fault location using unsynchronized two-terminal data," *IEEE Trans. Power Deliv*, vol. 31, no. 5, pp. 2296–2298, 2016.

[11] F. V. Lopes, K. M. Dantas, K. M. Silva, and F. B. Costa, "Accurate two-terminal transmission line fault location using traveling waves," *IEEE Transactions on Power Delivery*, vol. 33, no. 2, pp. 873–880, 2018.

[12] Y. Liu, G. Sheng, Z. He, and X. Jiang, "A traveling wave fault location method for earth faults based on mode propagation time delays of multi-measuring points," *Przegląd Elektrotechniczny (Electrical Review)*, vol. 88, pp. 254–258, 2012.

[13] H. W. Dommel and W. S. Meyer, "Computation of electromagnetic transients," *Proceedings of the IEEE*, vol. 62, no. 7, pp. 983–993, July 1974.

[14] E. O. Schweitzer, A. Guzmán, M. V. Mynam, V. Skendzic, B. Kasztenny, and S. Marx, "Locating faults by the traveling waves they launch," in *Protective Relay Engineers, 2014 67th Annual Conference for*. IEEE, 2014, pp. 95–110.

[15] K. Nanayakkara, A. Rajapakse, and R. Wachal, "Fault location in extra long hvdc transmission lines using continuous wavelet transform," in *International Conference on Power Systems Transients*, 2011, pp. 14–17.

[16] M. Ando, E. Schweitzer, and R. Baker, "Development and field-data evaluation of single-eng fault locator for two-thermal hvdv transmission lines part i: Data collection system and field data," *IEEE Transactions on Power Apparatus and Systems*, no. 12, pp. 3524–3530, 1985.

[17] ——, "Development and field-data evaluation of single-end fault locator for two-terminal hvdv transmission lines-part 2: Algorithm and evaluation," *IEEE transactions on power apparatus and systems*, no. 12, pp. 3531–3537, 1985.

[18] B. Kasztenny, A. Guzmán, N. Fischer, M. V. Mynam, and D. Taylor, "Practical setting considerations for protective relays that use incremental quantities and traveling waves," in *proceedings of the 43rd Annual Western Protective Relay Conference, Spokane, WA*, 2016.

[19] G. S. Luz, D. S. C. Junior, and S. G. Junior, "Hvdc transmission line modeling analysis in pscad and atp programs," in *XIII Symposium of Specialists in Electric Operational and Expansion Planning*, 2014.

[20] E. Schweitzer, A. Guzmán, M. Mynam, V. Skendzic, B. Kasztenny, C. Gallacher, and S. Marx, "Accurate single-end fault location and line-length estimation using traveling waves," in *13th International Conference on Developments in Power System Protection*, 2016.